Am J Physiol Cell Physiol 283: C93–C102, 2002.
First published March 6, 2002; 10.1152/ajpcell.00301.2001.

Adhesion of flowing monocytes to hypoxia-reoxygenation-exposed endothelial cells: role of Rac1, ROS, and VCAM-1

C. K. DOMINGOS NG,[1] SHAILESH S. DESHPANDE,[2]
KAIKOBAD IRANI,[2] AND B. RITA ALEVRIADOU[1]
[1]*Vascular Bioengineering Laboratory, Department of Biomedical Engineering, and* [2]*Division of Cardiology, Department of Medicine, Johns Hopkins University School of Medicine, Baltimore, Maryland 21205*

Received 2 July 2001; accepted in final form 28 February 2002

Ng, C. K. Domingos, Shailesh S. Deshpande, Kaikobad Irani, and B. Rita Alevriadou. Adhesion of flowing monocytes to hypoxia-reoxygenation-exposed endothelial cells: role of Rac1, ROS, and VCAM-1. *Am J Physiol Cell Physiol* 283: C93–C102, 2002. First published March 6, 2002; 10.1152/ajpcell.00301.2001.—Production of reactive oxygen species (ROS) by ischemic tissue after ischemia-reperfusion (I/RP) is an important factor that contributes to tissue injury. The small GTPase Rac1 mediates the oxidative burst, and ROS act on signaling pathways involved in expression of inflammatory genes. Because there is evidence implicating monocytes in the pathogenesis of I/RP injury, our objective was to determine the molecular mechanisms that regulate adhesive interactions between monocytes and hypoxia-reoxygenation (H/RO)-exposed cultured endothelial cells (ECs). When U937 cells were perfused over human umbilical vein ECs at 1 dyn/cm^2, H (1 h at 1% O_2)/RO (13 h) significantly increased the fluxes of rolling and stably adherent U937 cells. Either EC treatment with the antioxidant pyrrolidine dithiocarbamate (PDTC) or infection with AdRac1N17, which results in expression of the dominant-negative form of Rac1, abolished H/RO-induced ROS production, attenuated rolling, and abolished stable adhesion of U937 cells to H/RO-exposed ECs. Infection with AdRac1N17 also abolished H/RO-induced upregulation of vascular cell adhesion molecule (VCAM)-1. In turn, blocking VCAM-1 abolished U937 cell stable adhesion and slightly increased rolling. We concluded that the Rac1-dependent ROS partially regulate rolling and exclusively regulate stable adhesion of monocytic cells to ECs after H/RO and that stable adhesion, but not rolling, is mediated by ROS-induced expression of VCAM-1.

reactive oxygen species; shear stress; endothelial cell adhesion molecules

EARLY REPERFUSION is desirable after myocardial infarction, because it is an effective way to reduce infarct size and improve cardiac tissue function. However, reperfusion itself results in neutrophil adhesion in the postcapillary venules and emigration into the interstitium, increased monolayer permeability, and abnormal vasoregulation (16, 34). The pathogenesis of ischemia-reperfusion (I/RP) injury has been attributed to the production of oxygen-derived free radicals, often called reactive oxygen species (ROS), upon readmission of blood at reperfusion (19, 61). Vascular endothelial cells (ECs) are the primary target for ROS generated by themselves immediately after reperfusion and by adherent leukocytes at later times in reperfusion (43, 61).

In vitro hypoxia-reoxygenation (H/RO) studies with cultured ECs demonstrated that ROS production is increased shortly after reoxygenation (41, 53) and is dependent on activation of the small GTP-binding protein Rac1 (29). Rac1 regulates the activity of the transcription factor nuclear factor (NF)-κB via production of ROS (50), believed to occur through the plasma membrane-bound superoxide ($O_2^-\cdot$)-generating NAD(P)H oxidase (1). Under static conditions, neutrophil adhesion to anoxia (1 h)-reoxygenation (A/RO)-exposed human umbilical vein ECs (HUVECs) peaks at 30 and 240 min of reoxygenation: the early phase is mediated by transcription-independent upregulation of P-selectin and constitutively expressed intercellular adhesion molecule (ICAM)-1, and the late phase by transcription-dependent upregulation of E-selectin, P-selectin, and ICAM-1 (25). Both phases are ROS dependent, because adhesion is attenuated by EC treatment with the chemical antioxidant *N*-acetylcysteine (NAC) (30). The A/RO-induced activation of redox-sensitive transcription factors NF-κB and activator protein (AP)-1 promotes the late phase by stimulating the expression of EC adhesion molecules (30).

The fact that many EC adhesion molecules are upregulated after A/RO raised the possibility that the endothelium may support adhesion of other leukocyte subclasses, such as monocytes and lymphocytes, and that these cells may also mediate RP injury. In accordance with this, Kokura et al. (31) showed that T-lymphocyte adhesion to HUVECs increases after EC exposure to A (1 h)/RO (8 h) and that this hyperadhesivity is inhibited by antibodies against ICAM-1, vascular cell adhesion molecule (VCAM)-1, and their counterreceptors on T cells (β_2-integrins for ICAM-1 and α_4-integrins for VCAM-1). In addition, a number of in

Address for reprint requests and other correspondence: B. R. Alevriadou, Johns Hopkins Univ. School of Medicine, BME Dept., Traylor Bldg., Rm. 619, 720 Rutland Ave., Baltimore, MD 21205 (E-mail: ralevria@bme.jhu.edu).

The costs of publication of this article were defrayed in part by the payment of page charges. The article must therefore be hereby marked "*advertisement*" in accordance with 18 U.S.C. Section 1734 solely to indicate this fact.

vivo studies implicated monocytes in the pathogenesis of reperfusion injury. Birdsall et al. (6) found that ECs released monocyte chemoattractant protein (MCP)-1 that led to monocyte enrichment into the canine myocardium after reperfusion. Administration of an anti-MCP-1 antibody reduced infarct size in rat hearts (42). Blocking the function of endothelial monocyte-activating polypeptide (EMAP)-II prevented the onset of apoptosis and the influx of monocytes in reperfused kidney (12). Nevertheless, there is not yet an in vitro model that evaluates the molecular mechanisms of H/RO-induced monocyte adhesion to ECs.

Most in vitro studies on leukocyte adhesion to A/RO-exposed ECs have been conducted under static conditions (25, 30, 31), with few exceptions (17, 47). Incorporating flow in the adhesion assay provides a more realistic environment for adhesion to occur, in which flowing cells have to form contacts within milliseconds with their counterligands and to withstand the shearing forces imposed by the flow (32). Flow studies allow examination of the three types of adhesive interactions: tethering, rolling, and stable adhesion (39). In addition, EC-released inflammatory mediators are washed away by flow, preventing the buildup of soluble mediators and leaving only the surface-bound molecules active.

In light of the advantages of in vitro flow systems, we studied the adhesive interactions between human monocytic U937 cells and H/RO-exposed HUVECs under a wall shear stress of 1 dyn/cm^2, a level typically encountered in postcapillary venules (28, 49). Kukreti et al. (33) studied monocyte adhesion to interleukin (IL)-1β-stimulated ECs under flow and showed that L-selectin and α_4-integrins support rolling, whereas α_4- and β_2-integrins support stable adhesion. U937 cells are an appropriate model of monocytes in studying adherent interactions with ECs, because they express $\alpha_4\beta_1$- and β_2-integrins as well as L-selectin (22, 24, 26, 46). In A/RO-exposed HUVECs, VCAM-1 expression was shown to increase at 4 h after reoxygenation with a peak either at 12–16 h (57) or at 8 h (31). Because it remains unclear how and to what extent I/RP promotes monocyte adhesion, the objectives of the present study were *1*) to quantify the U937 cell adhesive interactions to H (1 h)/RO (13 h)-exposed HUVECs, *2*) to determine whether reoxygenation-induced ROS production promotes the expression of VCAM-1, *3*) to investigate whether Rac1 activation is required for reoxygenation-induced ROS production, and *4*) to clarify the role of VCAM-1 in monocytic cell-EC adhesive events.

Using the chemical antioxidant pyrrolidine dithiocarbamate (PDTC), which prevents NF-κB activation (37), we demonstrated that EC-derived ROS are involved both in VCAM-1 expression on H/RO-exposed HUVECs and in monocytic cell rolling and stable adhesion to these HUVECs. VCAM-1 was found to be solely responsible for stable adhesion, but it did not mediate rolling. The effects of H/RO exposure on VCAM-1 expression and U937 cell stable adhesion to H/RO-exposed ECs were completely blocked in ECs infected with an adenovirus that encodes a dominant-negative Rac1 (Rac1N17) but not with a control virus, suggesting that reoxygenation-induced ROS production is Rac1 dependent.

MATERIALS AND METHODS

U937 cell culture. U937 cells were purchased from American Type Culture Collection (ATCC, Rockville, MD) and cultured in RPMI 1640 with 25 mM HEPES (GIBCO BRL, Rockville, MD) supplemented with 10% heat-inactivated fetal bovine serum (FBS), 2 mM L-glutamine, 100 U/ml penicillin, and 100 μg/ml streptomycin (GIBCO). Cells were subcultured every 3 days until they reached a density of 10^6/ml in assay medium (RPMI 1640 with 25 mM HEPES and 1% FBS).

EC tissue culture. Primary noncryopreserved HUVECs were purchased from GlycoTech (Rockville, MD) and grown in T25 flasks in EGM-2 complete growth medium containing 2% FBS and growth supplements (Clonetics, San Diego, CA). On confluence, cells were rinsed, trypsinized (0.05% trypsin solution, Clonetics), and seeded in different containers, depending on the experimental protocol. All culture containers were coated with 0.2% gelatin (Sigma, St. Louis, MO). For monocyte adhesion assays, second-passage ECs were grown in 35-mm tissue culture dishes (Corning, Corning, NY). For cell-based ELISA, ECs of second to fourth passage were grown in 24-well plates (Becton Dickinson). For measurement of $O_2^-\cdot$ production, ECs of second to fourth passage were grown in 60-mm tissue culture dishes (Becton Dickinson).

EC infection with recombinant adenoviruses. The replication-deficient adenovirus AdRac1N17, which encodes the *myc* epitope-tagged dominant-negative allele of Rac1, was constructed with homologous recombination in HEK 293 cells as previously described (50). The control virus, AdβGal, which encodes the bacterial LacZ gene, was also described previously (51). Viruses were amplified in HEK-293 cells, purified on double cesium gradients, and plaque-titered (20). Purified AdRac1N17 and AdβGal had titers of 2×10^{10} and 5×10^{10} plaque-forming units (pfu)/ml, respectively. ECs were infected for 48 h before H/RO exposure (~80% confluence) at a multiplicity of infection (MOI) of 150 in EGM-2 complete growth medium. No obvious change on cell morphology was observed.

EC exposure to H/RO. Growth medium was removed, and a minimal amount of basal medium M199 (Gibco) was added in each container to decrease the diffusion distance for the atmospheric gases. Each container was exposed to a "hypoxic" gas mixture (5% CO_2-2% H_2-93% N_2; Puritan Bennett, Linthicum Heights, MD) in a humidified incubator (Billups-Rothenburg, Del Mar, CA) for 1 h. The incubator was flushed with N_2 at a pressure of 2 psi for 15 min before switching to the hypoxic gas mixture. To ensure an oxygen-free environment, the gas mixture was passed through a catalytic deoxygenator (Gas Purification Technology, Manalapan, NJ) before entry to the incubator. On measurement of the partial pressure of O_2 with a Clark-style probe (Hudson RCI, Temecula, CA) placed in the fluid contained in the tissue culture container, the starting partial pressure was 150 mmHg and dropped to 10 mmHg (1% O_2 content) within 10 min of hypoxia. Temperature inside the incubator was maintained at 37°C by a heating pad and was monitored throughout hypoxia. After 1 h of hypoxia, reoxygenation was initiated by returning the cells to the regular tissue culture incubator (normoxia: 21% O_2-5% CO_2-74% N_2). EGM-2 complete growth medium was added 30 min from the onset of reoxygenation to maintain cell viability. Cell viability was deter-

mined by trypan blue exclusion at 13 h from the onset of reoxygenation. Normoxic controls were exposed to normoxia for the duration of the experiment. PDTC (100 μM) was added to some monolayers 60 min before hypoxia. To some monolayers, a monoclonal antibody against VCAM-1 (1G11; Immunotech, Fullerton, CA), which was shown to inhibit U937 cell adhesion to tumor necrosis factor (TNF)-α-stimulated ECs (55), was added at a final concentration of 40 μg/ml for 30 min before completion of reoxygenation.

Cell-based ELISA for VCAM-1. At the end of 13-h reoxygenation or normoxia, VCAM-1 expression was determined by a cell-based ELISA. Briefly, monolayers were fixed with ice-cold ethanol for 10 min and nonspecific binding was blocked by adding I-block (Tropix, Bedford, MA) in PBS for 1 h at 37°C. Subsequently, 200 μl of mouse monoclonal anti-human VCAM-1 (1:2,500 dilution; R&D Systems, Minneapolis, MN) were added to each well and incubated overnight at 4°C. Monolayers were washed in PBS, incubated with biotin-conjugated goat anti-mouse IgG (1:2,500 dilution; Zymed, San Francisco, CA) in PBS for 1 h at room temperature, washed, and incubated with horseradish peroxidase (HRP)-conjugated streptavidin (1:5,000 dilution) in PBS for 30 min at room temperature. After washing with PBS, 200 μl of tetramethyl benzidine substrate solution (TMB; Sigma) were added to each well for 10 min. The reaction was stopped with 50 μl of 8 N H_2SO_4, and the plates were read on a spectrophotometric plate reader at 450 nm. The mean optical density (OD) of the wells containing normoxic cells without primary antibody was considered as background OD and was subtracted from all other readings. For each condition, measurement of triplicate wells was made to obtain an average value.

Flow adhesion assay. Each 35-mm tissue culture dish with a cell monolayer formed one side of a parallel-plate perfusion chamber (GlycoTech), with a flow path of 0.025-cm thickness and 0.1-cm width, as determined by a silicone gasket (GlycoTech). The tissue culture dish and the flow deck were kept together by vacuum. The perfusion chamber and inlet and outlet tubing were filled with assay medium and maintained at 37°C by a thermostatic air pump (Nikon, Garden City, NY). A syringe pump (Harvard Apparatus, South Natick, MA) was used to perfuse first assay medium for 2 min and then a suspension of U937 cells in assay medium for 5 min through the chamber at a constant flow rate of 0.64 ml/min. The viscosity of the assay medium was assumed to be 0.01 $g \cdot cm^{-1} \cdot s^{-1}$. By considering fully developed steady laminar flow of a viscous Newtonian fluid (5), the wall shear stress on the monolayer was calculated at 1 dyn/cm^2, as previously described (23, 49). The perfusion chamber was mounted on an inverted-stage microscope (Diaphot 300; Nikon) equipped with a video camera (CCD-72S; MTI, Michigan City, IN). Stage movement was controlled in the x and y directions with two micro-stepping motors (Multitech, West Chester, PA). For each experiment, three random microscopic fields (×20 objective, 0.38 mm^2/field) close to the chamber inlet were chosen for recording the U937 cell-EC adhesive interactions for 90 s per field with a JVC sVHS videocassette recorder (Professional Products, Baltimore, MD). Nine experimental conditions were tested by flow adhesion assay: 14-h normoxia (N); 1 h with PDTC and 14-h normoxia (N-PDTC); infection with AdβGal and 14-h normoxia (N-βGal); infection with AdRac1N17 and 14-h normoxia (N-Rac); 1-h hypoxia followed by 13-h reoxygenation (H/R); 1 h with PDTC and H (1 h)/RO (13 h) (H/R-PDTC); infection with AdβGal and H (1 h)/RO (13 h) (H/R-βGal); infection with AdRac1N17 and H (1 h)/RO (13 h) (H/R-Rac); and H (1 h)/RO (13 h) and 30 min with anti-VCAM-1 (H/R-VCAM).

Quantitation of monocytic cell-EC adhesive interactions. Video recordings from flow adhesion assays were digitized, and quantitative information was obtained by image processing (IC-300 modular image processing workstation; Inovision, Durham, NC). The total of U937 interacting cells per minute was defined as the number of cells that interacted with the monolayer in the digitized image (0.38 mm^2) for at least 1 s and included cells that tethered, rolled, and stably adhered. Brief contacts for <2 s were identified as tethering. Rolling cells were identified by acquiring "maximization" images for 3–5 s at 30 frames/s, as described previously (27). Rolling velocities in micrometers per second were determined by dividing the distances traveled by the acquisition time. Data from $n = 4$ independent experiments were pooled to give rolling velocities for 60 rolling monocytes for each condition tested. The frequency of occurrence for each velocity range was presented as a percentage relative to the total number of examined monocytes. Cells were defined as stably adherent if they remained attached to the monolayer for at least 5 s. Stably adherent cells were identified by acquiring "minimization" images for 5 s at 30 frames/s, as described previously (27), and were not included in the rolling cells. Distribution charts of the three interaction types were presented as a percentage of the total of interacting cells. Cells that interacted with other rolling or stably adherent cells before interacting with ECs were not accounted for, to study only primary adhesive events.

Measurement of EC ROS production. Lucigenin, a compound that emits light upon interaction with $O_2^-\cdot$ (21), was used to measure EC $O_2^-\cdot$ production, as described previously (4). Specifically, at 5 min of reoxygenation, ECs were harvested in PBS and cell pellets were suspended in a balanced salt solution consisting of (in mM) 130 NaCl, 5 KCl, 1 $MgCl_2$, 1 $CaCl_2 \cdot 2H_2O$, 35 H_3PO_4, and 20 HEPES, pH 7.4. The viability of the suspended cells was >95% as determined by trypan blue exclusion. EC suspensions were added at room temperature to triplicate wells of 96-well plates containing dark-adapted lucigenin (250 μM) in balanced salt solution. Increases in photon emission were measured every 20 s thereafter for 7 min in a scintillation counter (Top counter; Packard Instrument, Meriden, CT). Net increases in $O_2^-\cdot$ generation were calculated by comparison with a standard curve generated with xanthine/xanthine oxidase and normalized by protein content obtained from a protein assay (bicinchoninic acid; Pierce, Rockford, IL).

Statistical analysis. The number of cells per minute that tethered, rolled, or stably adhered are presented as means ± SE for $n = 4$ independent experiments in each condition. ODs from the ELISA assay were normalized to their corresponding normoxic controls and are presented as means ± SE for $n = 4$ independent experiments in each condition. Statistical significance of differences among means was determined using Statview software (Abacus Concepts, Berkeley, CA) to perform one-way ANOVA with Bonferroni corrections for multiple comparisons. P values ≤0.05 were considered significant.

RESULTS

U937 cell adhesion to H/RO-exposed ECs: role of ROS. Three types of adhesive interactions between U937 cells and ECs, namely, tethering, rolling, and stable adhesion, were quantified ($n = 4$; Fig. 1, *A–C*). Under normoxic conditions (N), tethering was the predominant type of interaction, accounting for 80% of total interacting cells (Fig. 1D). The interaction ap-

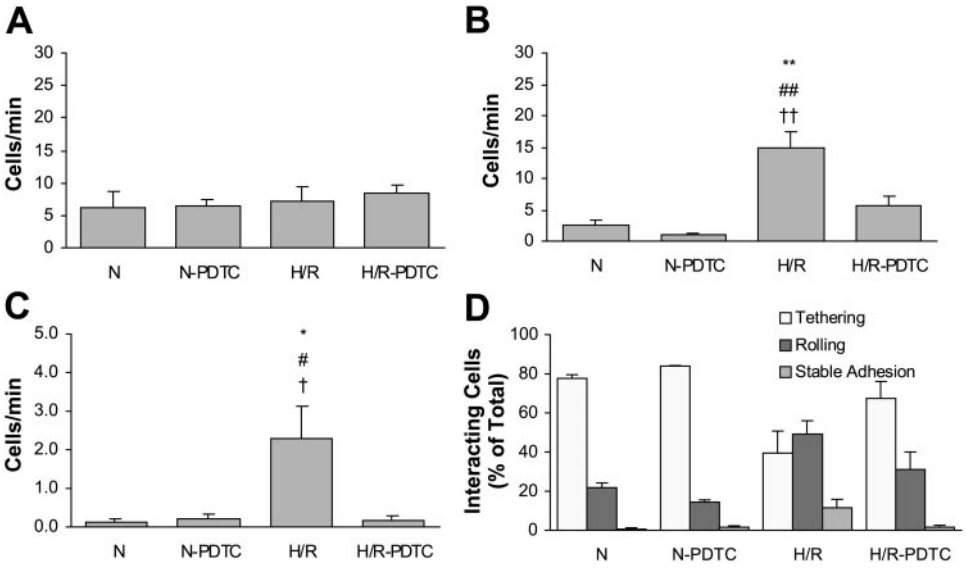

Fig. 1. Effects of pyrrolidine dithiocarbamate (PDTC) on monocytic cell adhesion to hypoxia-reoxygenation (H/RO)-exposed human umbilical vein endothelial cells (HUVECs) under a shear stress of 1 dyn/cm^2. Quantification of the flux of monocytic cell tethering (*A*), rolling (*B*), and stable adhesion (C) to the endothelial cell (EC) monolayers was performed under 4 conditions: 14-h normoxia (N); 1 h with PDTC (100 μM) and 14-h normoxia (N-PDTC); 1-h hypoxia followed by 13-h reoxygenation (H/R); and 1 h with PDTC and H (1 h)/RO (13 h) (H/R-PDTC). Cells per minute were measured in 3 random fields (area of 0.38 mm^2) for 90 s of recording/field. Bars represent means ± SE for $n = 4$ experiments. *$P <$ 0.05, **$P < 0.01$ vs. N; #$P < 0.05$, ##$P <$ 0.01 vs. N-PDTC; †$P < 0.05$, ††$P < 0.01$ vs. H/R-PDTC. *D*: distribution chart of the 3 types of adhesive interactions presented in the form of % total interacting cells.

peared to be nonspecific, because H (1 h)/RO (13 h) did not increase tethering (Fig. 1*A*). Under N, the frequency of rolling and stable adhesion accounted for 20% and 1%, respectively, of total interacting cells (Fig. 1*D*). H/RO-exposed ECs (H/R) were capable of supporting significantly higher fluxes of rolling and stably arrested cells: rolling increased 5.6-fold and stable adhesion increased from 0.1 to 2.3 cells/min, relative to N (Fig. 1, *B* and *C*). Rolling cells became the dominant interacting cell type after H/RO, accounting for >50% of total interacting cells compared with 20% under N (Fig. 1*D*). Almost all monocytes that were arrested onto the monolayer had previously rolled on it. The majority of rolling cells, however, later detached and reentered the fluid stream. Rolling cells appeared spherical, whereas many stably adherent cells were less regular in shape. Rarely, a stably adherent cell (cell arrested for at least 5 s) was later released and resumed rolling. No transmigrating cells were observed in these experiments.

To investigate the possible role of ROS in H/RO-induced monocyte adhesion, PDTC (100 μM) was incubated with ECs for 1 h before hypoxia. PDTC scavenges ROS by raising reduced glutathione levels inside the cells and was shown to inhibit NF-κB activation by preventing its mobilization (55). PDTC pretreatment of normoxic controls (N-PDTC) did not affect the flux of tethering or stably adherent cells compared with N ($n = 4$; Fig. 1, *A* and *C*). PDTC pretreatment decreased rolling, but the difference was not significant ($n = 4$; Fig. 1*B*). Moreover, PDTC significantly decreased rolling after H/RO (H/R-PDTC): the rolling flux dropped to 5.6 cell/min vs. 14.8 cells/min after H/RO (Fig. 1*B*). Compared with its normoxic counterpart (N-PDTC), the rolling flux was still 5-fold higher, resembling the 5.6-fold increase seen with the non-PDTC-treated pair (N, H/R). In contrast to rolling, the H/RO-induced increase in the flux of stably adherent cells was completely abolished by PDTC (Fig. 1*C*). In H/R-PDTC samples, the distribution of interactions returned to tethering dominant, as it was under N (>70%; Fig. 1*D*). It is possible that ROS regulate both the induction of adhesion molecule(s) that is (are) involved in H/RO-induced rolling and stable adhesion and even the expression of adhesion molecule(s) that is (are) involved in basal rolling.

Role of Rac1 in U937 cell adhesion to H/RO-exposed ECs. Because Rac1 is an integral part of the NAD(P)H oxidase complex and regulates ROS production in phagocytic and nonphagocytic cells (1, 29, 52), we asked whether monocytic cell adhesion to H/RO-exposed ECs was dependent on Rac1-mediated ROS production ($n = 4$; Fig. 2). Normoxic HUVECs infected with either AdRac1N17 (N-Rac) or AdβGal (N-βGal) showed the same distribution of the three types of U937 cell-EC adhesive interactions, as in noninfected N cells (Fig. 2*D*). Specifically for rolling and stable adhesion, there was no significant difference between N-Rac and N-βGal conditions (Fig. 2, *B* and *C*). For tethering, there was a decrease in N-Rac compared with N-βGal conditions, but it was not significant (Fig. 2*A*). After H/RO exposure of AdβGal-infected ECs (H/R-βGal), tethering was not affected (Fig. 2*A*). In contrast, H/R-βGal cells showed a 3- and 10-fold increase in rolling and stable adhesion, respectively (Fig. 2, *B* and *C*). In H/R-βGal cells, the distribution of interaction types was skewed toward rolling, with 50% of total interacting cells being rolling cells, as in noninfected H/R cells (Fig. 2*D*). Inhibition of Rac1 in H/RO-exposed ECs (H/R-Rac) significantly reduced the rolling flux by 62%, compared with its H/RO-exposed counterpart H/R-βGal (Fig. 2*B*). In H/R-Rac cells, the rolling flux was 1.7-fold higher than in N-Rac cells (Fig. 2*B*). Inhibition of Rac1 also resulted in complete inhibition of stable adhesion after H/RO (compare H/R-βGal and H/R-Rac, Fig. 2*C*). In H/R-Rac cells, the distribution of interaction types became as it was in N and H/R-PDTC cells (tethering accounted for 60% of total interacting cells; Fig. 2*D*). Hence, Rac1 activation may be required for rolling and stable adhesion after

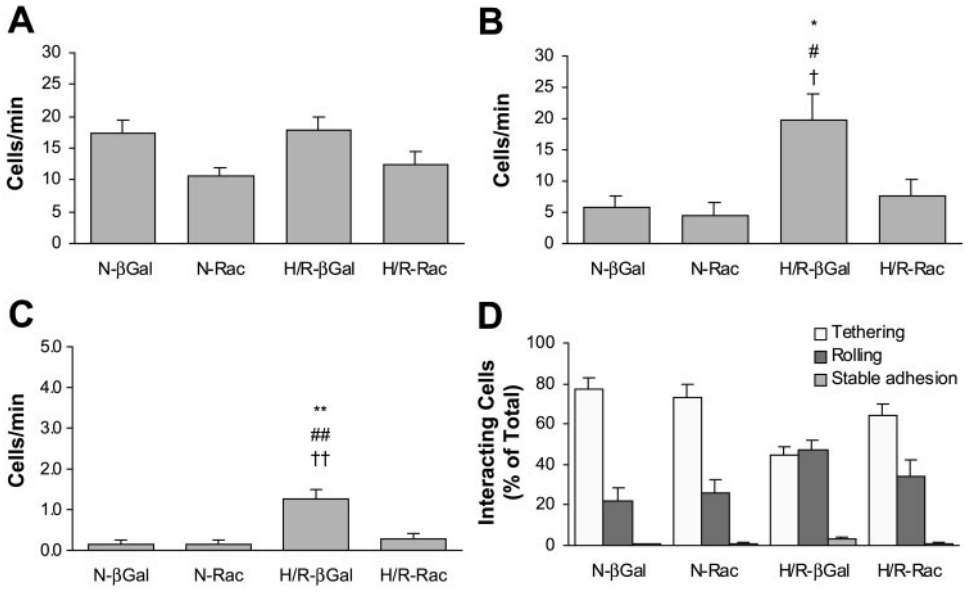

Fig. 2. Effects of adenoviral expression of dominant-negative Rac1 on monocytic cell adhesion to H/RO-exposed HUVECs under a shear stress of 1 dyn/cm^2. Quantification of the flux of monocytic cell tethering (*A*), rolling (*B*), and stable adhesion (*C*) to the EC monolayers was performed under 4 conditions: infection with AdβGal and 14-h normoxia (N-βGal); infection with AdRac1N17 and 14-h normoxia (N-Rac); infection with AdβGal and H (1 h)/RO (13 h) (H/R-βGal); and infection with AdRac1N17 and H (1 h)/RO (13 h) (H/R-Rac). All viruses were transfected at 150 multiplicity of infection (MOI) for 48 h before H/RO treatment. Cells per minute were measured in 3 random fields (area of 0.38 mm^2/field). Bars represent means ± SE ($n = 4$). *$P < 0.05$, **$P < 0.01$ vs. N-βGal; #$P < 0.05$, ##$P < 0.01$ vs. N-Rac; †$P < 0.05$, ††$P < 0.01$ vs. H/R-Rac. *D*: distribution chart of the 3 types of adhesive interactions presented in the form of % total interacting cells.

H/RO but is not required for adhesive interactions under normoxia (both N-βGal and N-Rac showed the same rates of tethering, rolling, and stable adhesion).

EC $O_2^-\cdot$ generation after H/RO. The effects of PDTC treatment or Rac1 inhibition on H/RO-induced EC $O_2^-\cdot$ generation were studied by lucigenin chemiluminescence at 5 min after reoxygenation. A characteristic run, from two identical runs, is shown in Fig. 3. Under normoxia, there was a low basal level of $O_2^-\cdot$ generation that was slightly affected by PDTC treatment or AdβGal infection. AdRac1N17 infection led to even lower basal $O_2^-\cdot$ production (60% compared with N). EC $O_2^-\cdot$ generation increased more than twofold in both H/R and H/R-βGal cells, suggesting that $O_2^-\cdot$ is one ROS that is greatly overproduced shortly after reoxygenation. Either PDTC treatment (H/R-PDTC) or infection with AdRac1N17 (H/R-Rac) markedly, but not completely, blocked the H/RO-induced increase in $O_2^-\cdot$ production (Fig. 3). The changes in $O_2^-\cdot$ production under different conditions appear to correspond to changes in U937 cell rolling and stable adhesion, suggesting that H/RO-induced $O_2^-\cdot$ production may play a role in the expression of EC adhesion molecules for monocytes.

EC VCAM-1 expression after H/RO. Because VCAM-1 is involved in monocyte-EC adhesive events under flow (33) and is known to be upregulated by H/RO (31, 57), we studied EC VCAM-1 expression under different conditions by cell ELISA ($n = 4$; Fig. 4). In N-βGal cells, there was a slight, but not significant, increase in VCAM-1 expression compared with N cells. Either PDTC treatment (N-PDTC) or infection with AdRac1N17 (N-Rac) downregulated the basal VCAM-1 expression compared with that of their respective controls (N, N-βGal), but the difference was not significant. Exposure to H/RO increased VCAM-1 expression almost twofold in both infected and noninfected cells. PDTC treatment (H/R-PDTC) inhibited by 75% and infection

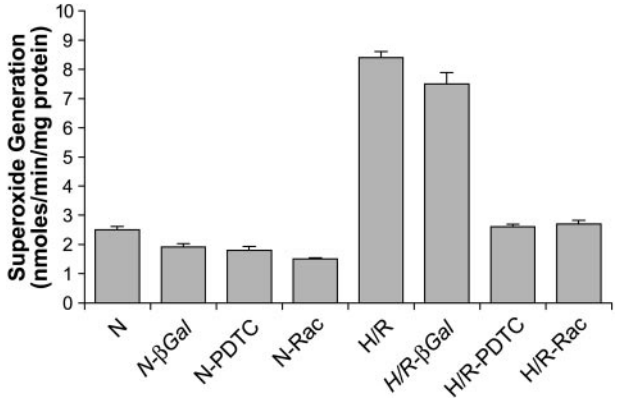

Fig. 3. Superoxide generation by cultured HUVECs exposed to different treatments, as measured by lucigenin-amplified chemiluminescence. Bars represent means ± SE. One of two experiments with identical results is shown.

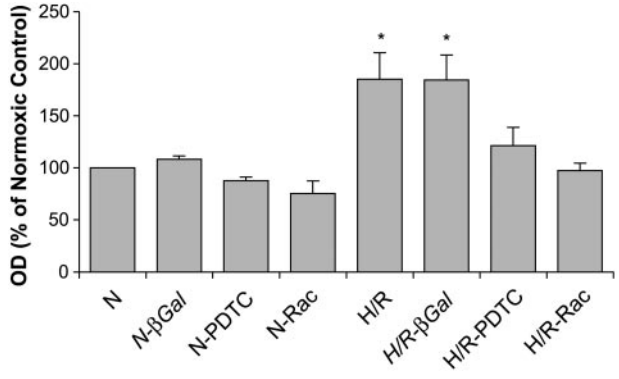

Fig. 4. Surface vascular cell adhesion molecule (VCAM)-1 expression on HUVECs exposed to different treatments as quantified by whole cell ELISA with an anti-VCAM-1 antibody. Data are presented as the percentage of optical density (OD) in response to each treatment relative to the normoxic control (N). Bars represent means ± SE for $n = 4$ experiments. *$P < 0.05$ vs. N, N-βGal, N-PDTC, N-Rac, and H/R-Rac.

with AdRac1N17 (H/R-Rac) almost completely abolished the H/RO-induced increase in VCAM-1 expression compared with H/R and H/R-βGal, respectively (Fig. 4). Thus H/RO-induced VCAM-1 expression is regulated by Rac1-dependent ROS.

Role of VCAM-1 in U937 cell adhesion to H/RO-exposed ECs. Because VCAM-1 supports monocyte stable adhesion to cytokine-stimulated ECs (33) and has been implicated in tethering and rolling (2, 3, 33), we studied the VCAM-1 contribution to U937 cell adhesive interactions with H/RO-exposed ECs by using a blocking anti-VCAM-1 monoclonal antibody ($n = 4$; Fig. 5). Incubation with anti-VCAM-1 antibody 1G11 (40 μg/ml) for 30 min before completion of 13 h of reoxygenation (H/R-VCAM) did not affect the tethering flux (Fig. 5*A*). Incubation with anti-VCAM-1 antibody resulted in a measurable (40%), but not significant, increase in rolling flux compared with H/R (Fig. 5*B*). Furthermore, it completely abolished H/RO-induced stable adhesion, indicating a crucial role of VCAM-1 in monocytic cell stable adhesion (Fig. 5*C*). The shift in distribution of interaction types from tethering to rolling, observed in H/R, was maintained in H/R-VCAM, with rolling accounting for >60% of total interactions (Fig. 5*D*). In H/R-VCAM, not only did the flux of rolling cells increase compared with H/R (Fig. 5*B*), but the mean rolling velocity also slightly decreased. Figure 6 shows the distribution of rolling velocities of U937 cells perfused at 1 dyn/cm^2 over ECs exposed to different conditions (N, H/R, or H/R-VCAM; $n = 4$). Under N conditions, cells rolled at a mean rolling velocity of 133 ± 8 μm/s (±SE; Fig. 6*A*). H/R caused cells to roll significantly more slowly, at 88 ± 8 μm/s on average (±SE; Fig. 6*B*). H/R-VCAM resulted in further skewing of the distribution of rolling velocities to the low side: the mean rolling velocity was 79 ± 8 μm/s (±SE; Fig. 6*C*), which was significantly different from N but not significantly different from H/R.

DISCUSSION

The present study provides the first evidence that *1*) flowing monocytic cells will roll and firmly adhere to H/RO-exposed ECs, *2*) stable adhesion is totally, and rolling partially, dependent on Rac1-mediated ROS production, and *3*) VCAM-1 mediates stable adhesion, but not rolling, of monocytic cells to H/RO-exposed ECs. By incorporating flow in the adhesion assay, it is possible not only to observe and quantify each step in the cascade of adhesive events (tethering, rolling, and stable adhesion) but also to determine the molecular mechanisms that regulate individual steps.

Tethering was the most prominent adhesive interaction type under normoxia (Fig. 1*D*). These brief contacts of monocytic cells with HUVEC monolayers cause a temporary halt in the movement of flowing cells, and although most are instantly released back to the fluid stream, some start to roll on the EC surface. Rolling decelerates the monocytes, allowing them to sample the local environment and interact with EC receptors that mediate firm arrest. A limited flux of stably adherent cells was observed under N conditions (Fig. 1*C*). EC exposure to H (1 h)/RO (13 h) significantly increased the fluxes of rolling and stably adherent cells, compared with N, while maintaining the same tethering flux (Fig. 1, *A–C*). Rolling and stable adhesion fluxes increase when monocytes are perfused over cytokine-stimulated ECs (33, 36). The flux of stably adherent U937 cells to H/RO-exposed HUVECs was low (~5 cells·mm^{-2}·min^{-1} at 1 dyn/cm^2) compared with that of human peripheral blood monocytes to either 4-h IL-1β-stimulated HUVECs (~15 cells·mm^{-2}·min^{-1} at 2 dyn/cm^2; Ref. 33) or 24-h IL-4-stimulated HUVECs (~60 cells·mm^{-2}·min^{-1} at 0.8 dyn/cm^2) (36). Consistent with this finding, Kokura et al. (31) showed that A (1 h)/RO (8 h) induces an increase in (static) T-lympho-

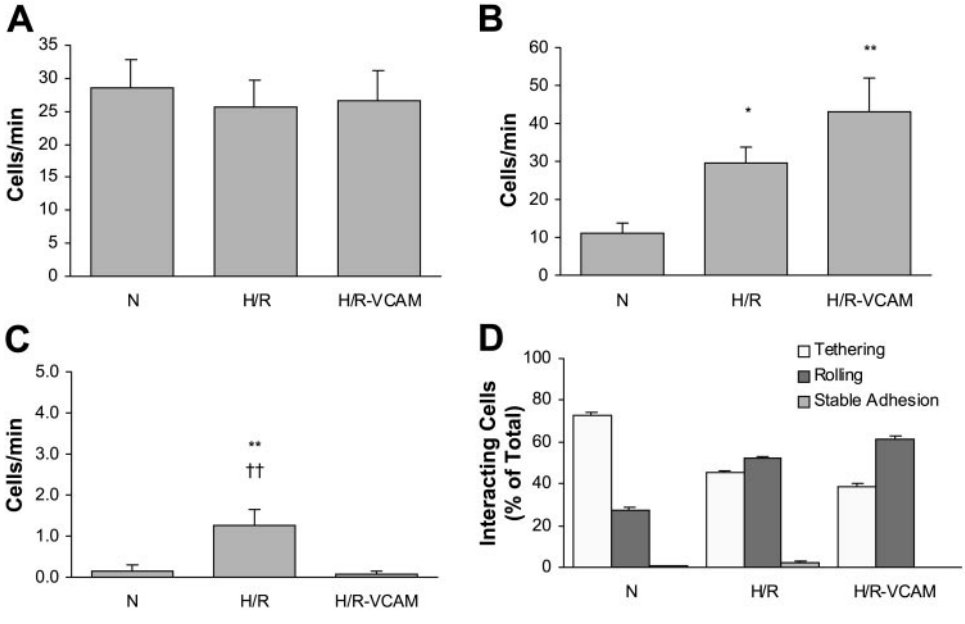

Fig. 5. Effects of a blocking monoclonal antibody against VCAM-1 on U937 cell adhesion to H/RO-exposed HUVECs under a shear stress of 1 dyn/cm^2. Quantification of the monocytic cell flux of tethering (*A*), rolling (*B*), and stable adhesion (*C*) to the EC monolayers under 3 different conditions: N, H/R, and H (1 h)/RO (13 h) and 30 min with anti-VCAM-1 antibody 1G11 (40 μg/ml) (H/R-VCAM). Cells per minute were measured in 3 random fields (area of 0.38 mm^2 each). Bars represent means ± SE ($n = 4$ experiments). *$P < 0.05$, **$P <$ 0.01 vs. N; ††$P < 0.01$ vs. H/R-VCAM. *D*: distribution chart of the 3 types of adhesive interactions presented in the form of % total interacting cells.

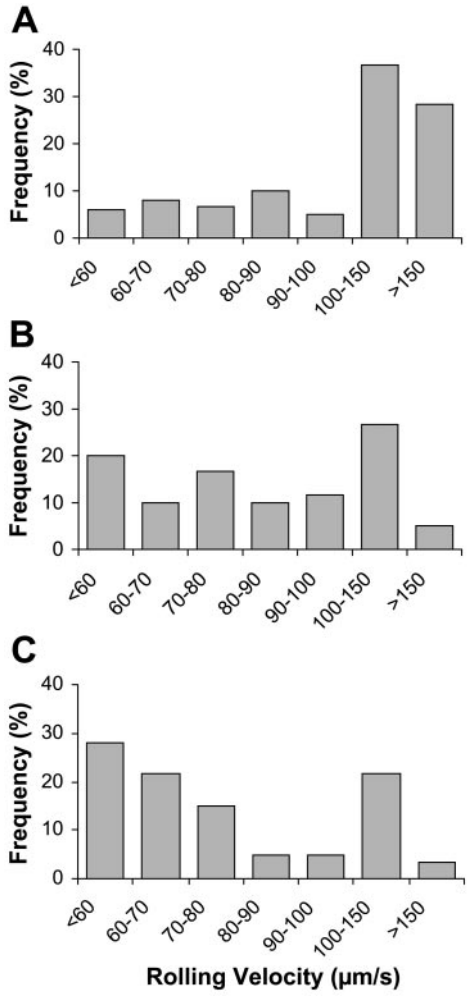

Fig. 6. Distribution of U937 cell rolling velocities when a monocytic cell suspension was perfused over normoxic HUVECs (*A*), H (1 h)/RO (13 h)-exposed HUVECs (*B*), and H (1 h)/RO (13 h)-exposed HUVECs that were incubated with anti-VCAM-1 antibody 1G11 (40 μg/ml) for the last 30 min of reoxygenation (*C*) under a shear stress of 1 dyn/cm^2. Frequencies are expressed as % total examined monocytes (60 monocytes were examined in each case). Data from 1 characteristic experiment of 2 with similar results are shown.

cyte adhesion of a magnitude similar to the response induced by lower levels of cytokine exposure.

EC $O_2^-\cdot$ generation increased shortly after reoxygenation (Fig. 3), in agreement with data on H/RO-induced ROS production monitored by the oxidant-sensitive fluorescent probes 2,7-dichlorofluorescein diacetate and dihydrorhodamine 123 (9, 29). The fact that treatment with PDTC or infection with AdRac1N17 attenuated, without blocking completely, the H/RO-induced $O_2^-\cdot$ generation implies that there are intracellular, e.g., mitochondrial, ROS sources inaccessible by PDTC and H/RO-stimulated $O_2^-\cdot$-generating pathways independent of Rac1. The degree of inhibition of $O_2^-\cdot$ production in H/R-PDTC was slightly higher than that in H/R-Rac (81% vs. 72%) compared with corresponding controls (Fig. 3). This suggests that *1*) PDTC treatment probably eliminates most of the $O_2^-\cdot$ generated by the Rac1-regulated oxidase and *2*) the Rac1-regulated oxidase is the main source of $O_2^-\cdot$ generation upon EC stimulation by H/RO. However, because ECs were infected with AdRac1N17 at a MOI of 150 and higher MOI were not tried (≤200; Ref. 13), there is also a possibility that Rac1N17 expression may have not blocked the NAD(P)H oxidase activity entirely.

EC treatment with PDTC significantly attenuated H/RO-induced rolling and completely abolished stable adhesion (Fig. 1, *B* and *C*), suggesting that ROS regulate monocytic cell rolling and stable adhesion to H/RO-exposed ECs. PDTC also decreased rolling under N, but the difference was not significant (Fig. 1*B*), implying that ROS may, in part, regulate the expression of a constitutively expressed adhesion molecule involved in rolling. Normoxic ECs infected with either AdRac1N17 or AdβGal showed the same rolling and stable adhesion fluxes and similar tethering fluxes (Fig. 2). Infection with AdRac1N17 significantly reduced the H/RO-induced increase in rolling and completely abolished the H/RO-induced increase in stable adhesion compared with H/RO-exposed ECs infected with AdβGal (Fig. 2), suggesting that the Rac1-dependent ROS mainly regulate monocytic cell rolling and exclusively regulate stable adhesion. Specifically for rolling, AdRac1N17 was more potent than PDTC in attenuating H/RO-induced rolling, compared with their respective N counterparts (1.7-fold with H/R-Rac vs. 3.4-fold with H/R-βGal; 5-fold with H/R-PDTC vs. 5.6-fold with H/R). This implies that Rac1-regulated ROS-independent signaling pathways contribute to the H/RO-induced increase in rolling. Similarly, chemical antioxidants were shown to be effective at suppressing H/RO-induced heat shock factor (HSF) activation but not as effective as Rac1N17, implying that Rac1-dependent ROS-independent mechanisms partially regulate HSF-mediated transcription (44), leading to attenuation of proinflammatory responses (54).

From the measurements of EC viability at 13 h of reoxygenation (complete growth medium was added back to ECs at 30 min of reoxygenation), the adhesive interactions between a fraction of ECs in the monolayer and U937 cells are not due to EC death. Neither PDTC nor Rac1 inhibition, with or without H/RO exposure, caused cell death, because >90% cells were viable in each case. Furthermore, the continuation of the monolayers was always checked under the microscope right before the flow adhesion assay. In accordance with this, there is evidence that *1*) EC infection with AdRac1N17 at MOIs of 50–200 does not cause apoptosis (13), *2*) incubation of confluent HUVECs with PDTC (100 μM) for 24 h does not induce cell death (14), and *3*) infection with AdRac1N17 protects HUVECs from H/RO-induced cell death (29). Hence, although we have not tested specifically for apoptosis, we know that our studies were performed with viable ECs.

Because VCAM-1 mediates monocyte adhesive interactions with cytokine-stimulated ECs under flow (33) and antioxidants inhibit NF-κB activation and VCAM-1 expression on cytokine-stimulated ECs (37, 55), we evaluated the effect of H/RO, and the importance of H/RO-induced Rac1-dependent ROS, on VCAM-1 ex-

pression. In agreement with published studies on the time course of VCAM-1 on HUVECs exposed to A (1 or 4 h)/RO (31, 57), we found a twofold increase in VCAM-1 expression at 13 h of reoxygenation (Fig. 4). H/RO-induced VCAM-1 upregulation was significantly attenuated by PDTC and almost completely abolished by AdRac1N17 (Fig. 4), suggesting that VCAM-1 expression is mainly regulated by Rac1-dependent ROS. NF-κB and, to a lesser extent, AP-1 are involved in A/RO-induced VCAM-1 expression (31). Because Rac1-mediated ROS are a major part of total ROS (Fig. 3) and both NF-κB DNA binding activity and the turnover of the inhibitor IκB are oxidant sensitive (18), it is possible that Rac1-mediated ROS regulate NF-κB-driven gene expression. There are downstream effectors of Rac1, however, that may also be important in regulating H/RO-induced expression of VCAM-1: Rac1 has been implicated in activation of members of the family of mitogen-activated protein (MAP) kinases, such as p38 (60) and the extracellular signal-regulated kinases (ERK1/2) (59), and these MAP kinases are required for NF-κB-driven gene expression (7, 8). The GTPases Rac1 and Cdc42 are also known to regulate a protein kinase cascade initiated at p21-activated kinase (Pak)-1 and leading to activation of c-Jun NH_2-terminal kinase (JNK) and p38 MAP kinase (10, 60). Hence, it is possible that each of the above effectors, as well as the actin cytoskeleton (11), differentially regulate VCAM-1 expression.

Because blocking VCAM-1 completely abolished firm adhesion (Fig. 5*C*), VCAM-1 is the sole mediator of monocytic cell firm adhesion to H/RO-exposed HUVECs. This agrees with the fact that blocking $\alpha_4\beta_1$ significantly reduced firm adhesion of flowing monocytes to IL-1β-stimulated HUVECs, whereas blocking β_2-integrins (hence, ICAM-1-mediated pathway) did not (33). A limited number of U937 cells were arrested on H/RO-exposed ECs without prior rolling, suggesting that VCAM-1 is capable of firm adhesion even in the absence of selectin-mediated adhesive interactions. The $\alpha_4\beta_1$-VCAM-1 interaction can precede activation events that are required for development of firm adhesion (2, 15, 58). From our findings, however, VCAM-1 does not mediate tethering or rolling (Fig. 5, *A* and *B*). The surface density of VCAM-1 after H/RO, despite being higher than basal, may not be high enough to increase the avidity between $\alpha_4\beta_1$ and VCAM-1 to mediate tethering or rolling.

Rolling markedly increased in the presence of saturating concentrations of anti-VCAM-1 antibody compared with H/R (Fig. 5*B*). Increased rolling flux may be due to decreased firm adhesion upstream of the field of view, thus more rolling cells enter the field per unit time. This agrees with the data of Weber et al. (56), who inhibited NF-κB mobilization by overexpression of IκB in HUVECs and found that reduced induction of VCAM-1/ICAM-1 by TNF-α resulted in a decrease in the ability of monocytes to firmly adhere and an increase in the rolling fraction of monocytes. However, in our case, the increase in rolling cells after VCAM-1 blockade cannot be accounted for solely by the reduction in stably adherent cells, as can be seen by comparing Fig. 5, *B* and *C*. The increased flux of rolling monocytes combined with the reduced rolling velocities after VCAM-1 blockade (Fig. 6) suggest a greater number of receptor-ligand bonds. Antibody cross-linking of VCAM-1 on the EC surface induces a Ca^{2+} flux (48) and activates NAD(P)H oxidase to produce ROS (38). Hence, VCAM-1-mediated outside-in signaling may cause rapid expression of the oxidant-sensitive preformed P-selectin from Weibel-Palade bodies (45), or of a novel receptor, leading to increased rolling interactions and reduced rolling velocities.

The U937 cell mean rolling velocity over H/RO-exposed HUVECs is comparable to that of monocytes over (24 h) IL-4-stimulated HUVECs (36) but is higher than that of monocytes over either (4 h) IL-1β- or (6 h) TNF-α-activated HUVECs (33, 35). Rolling is probably mediated by L-selectin binding to sialylated determinants on the EC surface, as in the case of monocytes rolling over IL-1β-stimulated HUVECs (33). At 13 h of reoxygenation, P- and E-selectin are not likely to be present on the EC surface, because their expression levels were shown to return to basal levels at 10 h of reoxygenation (25) and neither of the two affected static T-lymphocyte adhesion at 8 h of reoxygenation (31).

Under our experimental conditions, besides exposure to hypoxia, ECs were exposed to serum/growth factor deprivation for 1 h during hypoxia (and the first 30 min of reoxygenation), to make hypoxia more physiologically relevant to ischemia. Because of the short time period of serum/growth factor withdrawal, it is believed that the effects of our treatment on EC signaling and EC-leukocyte adhesive events are for the most part due to H/RO exposure. In sum, we demonstrated that flowing monocytic cells tether, roll, and firmly adhere to cultured HUVECs exposed to H/RO. EC Rac1-dependent ROS partially regulate rolling and exclusively regulate stable adhesion. Stable adhesion, but not rolling, is mediated by induction of VCAM-1 expression. In vivo, physical and biological factors not present in our in vitro system may modulate leukocyte adhesion within the range of physiological shear stresses (40). In vitro systems, however, are still very useful in subjecting cultured ECs to well-defined flow conditions and in understanding the molecular basis underlying the leukocyte response to ECs after I/RP injury.

We thank A. Hall for the Rac1N17 cDNA, R. Crystal and T. Finkel for AdβGal, and J. T. Patton for helpful discussions.

B. R. Alevriadou was supported by National Heart, Lung, and Blood Institute Grant HL-54089, a Whitaker Biomedical Engineering research grant, and a grant from the Johns Hopkins Medical Institutions Center for Advanced Transfusion Practices and Blood Research. K. Irani was supported by a Johns Hopkins Clinician Scientist Award, the American Heart Association, the Bernard Foundation, and an endowment from Abraham and Virginia Weiss.

REFERENCES

1. **Abo A, Pick E, Hall A, Totty N, Teahan CG, and Segal AW.** Activation of the NADPH oxidase involves the small GTP-binding protein p21rac1. *Nature* 353: 668–670, 1991.

2. **Alon R, Kassner PD, Woldemar Carr M, Finger EB, Hemler ME, and Springer TA.** The integrin VLA-4 supports tethering and rolling in flow on VCAM-1. *J Cell Biol* 128: 1243–1253, 1995.
3. **Berlin C, Bargatze RF, Campbell JJ, von Andrian UH, Szabo MC, Hasslen SR, Nelson RD, Berg EL, Erlandsen SL, and Butcher EC.** α_4 Integrins mediate lymphocyte attachment and rolling under physiologic flow. *Cell* 80: 413–422, 1995.
4. **Bhunia AK, Arai T, Bulkley G, and Chatterjee S.** Lactosylceramide mediates tumor necrosis factor-alpha-induced intercellular adhesion molecule-1 (ICAM-1) expression and the adhesion of neutrophil in human umbilical vein endothelial cells. *J Biol Chem* 273: 34349–34357, 1998.
5. **Bird RB, Stewart WE, and Lightfoot EN.** *Transport Phenomena.* New York: Wiley, 1960.
6. **Birdsall HH, Green DM, Trial J, Youker KA, Burns AR, MacKay CR, LaRosa GJ, Hawkins HK, Smith CW, Michael LH, Entman ML, and Rossen RD.** Complement C5a, TGF-beta 1, and MCP-1, in sequence, induce migration of monocytes into ischemic canine myocardium within the first one to five hours after reperfusion. *Circulation* 95: 684–692, 1997.
7. **Carter AB and Hunninghake GW.** A constitutive active MEK→ERK pathway negatively regulates NF-kappa B-dependent gene expression by modulating TATA-binding protein phosphorylation. *J Biol Chem* 275: 27858–27864, 2000.
8. **Carter AB, Knudtson KL, Monick MM, and Hunninghake GW.** The p38 mitogen-activated protein kinase is required for NF-kappaB-dependent gene expression. The role of TATA-binding protein (TBP). *J Biol Chem* 274: 30858–30863, 1999.
9. **Cepinskas G, Lush CW, and Kvietys PR.** Anoxia/reoxygenation-induced tolerance with respect to polymorphonuclear leukocyte adhesion to cultured endothelial cells. A nuclear factor-kappaB-mediated phenomenon. *Circ Res* 84: 103–112, 1999.
10. **Coso OA, Chiariello M, Yu JC, Teramoto H, Crespo P, Xu N, Miki T, and Gutkind JS.** The small GTP-binding proteins Rac1 and Cdc42 regulate the activity of the JNK/SAPK signaling pathway. *Cell* 81: 1137–1146, 1995.
11. **Crawford LE, Milliken EE, Irani K, Zweier JL, Becker LC, Johnson TM, Eissa NT, Crystal RG, Finkel T, and Goldschmidt-Clermont PJ.** Superoxide-mediated actin response in post-hypoxic endothelial cells. *J Biol Chem* 271: 26863–26867, 1996.
12. **Daemen MA, van't Veer C, Denecker G, Heemskert VH, Wolfs TG, Clauss M, Vandenabeele P, and Buurman WA.** Inhibition of apoptosis induced by ischemia-reperfusion prevents inflammation. *J Clin Invest* 104: 541–549, 1999.
13. **Deshpande SS, Angkeow P, Huang J, Ozaki M, and Irani K.** Rac1 inhibits TNF-alpha-induced endothelial cell apoptosis: dual regulation by reactive oxygen species. *FASEB J* 14: 1705–1714, 2000.
14. **Erl W, Weber C, and Hansson GK.** Pyrrolidine dithiocarbamate-induced apoptosis depends on cell type, density, and the presence of Cu^{2+} and Zn^{2+}. *Am J Physiol Cell Physiol* 278: C1116–C1125, 2000.
15. **Gerszten RE, Lim YC, Ding HT, Snapp K, Kansas G, Dichek DA, Cabanas C, Sanchez-Madrid F, Gimbrone MA Jr, Rosenzweig A, and Luscinskas FW.** Adhesion of monocytes to vascular cell adhesion molecule-1-transduced human endothelial cells. Implications for atherogenesis. *Circ Res* 82: 871–878, 1998.
16. **Granger DN and Korthuis RJ.** Physiologic mechanisms of post-ischemic tissue injury. *Annu Rev Physiol* 57: 311–332, 1995.
17. **Granger DN, Kvietys PR, and Perry MA.** Leukocyte-endothelial cell adhesion induced by ischemia and reperfusion. *Can J Physiol Pharmacol* 71: 67–75, 1993.
18. **Griendling KK, Sorescu D, Lasseque B, and Ushio-Fukai M.** Modulation of protein kinase activity and gene expression by reactive oxygen species and their role in vascular physiology and pathophysiology. *Arterioscler Thromb Vasc Biol* 20: 2175–2183, 2000.
19. **Grisham MB, Granger DN, and Lefer DJ.** Modulation of leukocyte-endothelial interactions by reactive metabolites of oxygen and nitrogen: relevance to ischemic heart disease. *Free Radic Biol Med* 25: 404–433, 1998.
20. **Guzman RJ, Hirschowitz EA, Brody SL, Crystal RG, Epstein SE, and Finkel T.** In vivo suppression of injury-induced vascular smooth muscle cell accumulation using adenovirus-mediated transfer of the herpes simplex virus thymidine kinase gene. *Proc Natl Acad Sci USA* 91: 10732–10726, 1994.
21. **Gyllenhammar H.** Lucigenin chemiluminescence in the assessment of neutrophil superoxide production. *J Immunol Methods* 97: 209–213, 1987.
22. **Hauser IA, Johnson DR, and Madri JA.** Differential induction of VCAM-1 on human iliac venous and arterial endothelial cells and its role in adhesion. *J Immunol* 151: 5172–5185, 1993.
23. **Hinds MT, Park YJ, Jones SA, Giddens DP, and Alevriadou BR.** Local hemodynamics affect monocytic cell adhesion to a three-dimensional flow model coated with E-selectin. *J Biomech* 34: 95–103, 2001.
24. **Huo Y, Hafezi-Moghadam A, and Ley K.** Role of vascular cell adhesion molecule-1 and fibronectin connecting segment-1 in monocyte rolling and adhesion on early atherosclerotic lesions. *Circ Res* 87: 153–159, 2000.
25. **Ichikawa H, Flores S, Kvietys PR, Wolf RE, Yoshikawa T, Granger DN, and Aw TY.** Molecular mechanisms of anoxia/reoxygenation-induced neutrophil adherence to cultured endothelial cells. *Circ Res* 81: 922–931, 1997.
26. **Islam KN, Devaraj S, and Jialal I.** α-Tocopherol enrichment of monocytes decreases agonist-induced adhesion to human endothelial cells. *Circulation* 98: 2255–2261, 1998.
27. **Jones DA, Abbassi O, McIntire LV, McEver RP, and Smith CW.** P-selectin mediates neutrophil rolling on histamine-stimulated endothelial cells. *Biophys J* 65: 1560–1569, 1993.
28. **Jones DA, Smith CW, and McIntire LV.** Effects of fluid shear stress on leukocyte adhesion to endothelial cells. In: *Physiology and Pathophysiology of Leukocyte Adhesion*, edited by Granger DN and Schmid-Schonbein GW. New York: Oxford Univ. Press, 1995, p. 148–168.
29. **Kim KS, Takeda K, Sethi R, Pracyk JB, Tanaka K, Zhou YF, Yu ZX, Ferrans VJ, Bruder JT, Kovesdi I, Irani K, Goldschmidt-Clermont P, and Finkel T.** Protection from reoxygenation injury by inhibition of rac1. *J Clin Invest* 101: 1821–1826, 1998.
30. **Kokura S, Wolf RE, Yoshikawa T, Granger DN, and Aw TY.** Molecular mechanisms of neutrophil-endothelial cell adhesion induced by redox imbalance. *Circ Res* 84: 516–524, 1999.
31. **Kokura S, Wolf RE, Yoshikawa T, Ichikawa H, Granger DN, and Aw TY.** Endothelial cells exposed to anoxia/reoxygenation are hyperadhesive to T-lymphocytes: kinetics and molecular mechanisms. *Microcirculation* 7: 13–23, 2000.
32. **Konstantopoulos K and McIntire LV.** Effects of fluid dynamic forces on vascular cell adhesion. *J Clin Invest* 100: S19–S23, 1997.
33. **Kukreti S, Konstantopoulos K, Smith CW, and McIntire LV.** Molecular mechanisms of monocyte adhesion to interleukin-1beta-stimulated endothelial cells under physiologic flow conditions. *Blood* 89: 4104–4111, 1997.
34. **Kvietys PR, Cepinskas G, and Granger DN.** Neutrophil-endothelial cell interactions during ischemia/reperfusion. In: *Tissue Perfusion and Organ Function: Ischemia/Reperfusion Injury*, edited by Kamada T, Shiga T, and McCuskey RS. Amsterdam: Elsevier, 1996, p. 179–191.
35. **Luscinskas FW, Ding H, Tan P, Cumming D, Tedder TF, and Gerritsen ME.** L- and P-selectins, but not CD49d (VLA-4) integrins, mediate monocyte initial attachment to TNF-alpha-activated vascular endothelium under flow in vitro. *J Immunol* 157: 326–335, 1996.
36. **Luscinskas FW, Kansas GS, Ding H, Pizcueta P, Schleiffenbaum BE, Tedder TF, and Gimbrone MA Jr.** Monocyte rolling, arrest and spreading on IL-4-activated vascular endothelium under flow is mediated via sequential action of L-selectin, beta 1-integrins, and beta 2-integrins. *J Cell Biol* 125: 1417–1427, 1994.
37. **Marui N, Offermann MK, Swerlick R, Kunsch C, Rosen CA, Ahmad M, Alexander RW, and Medford RM.** Vascular cell adhesion molecule-1 (VCAM-1) gene transcription and expression are regulated through an antioxidant-sensitive mecha-

nism in human vascular endothelial cells. *J Clin Invest* 92: 1866–1874, 1993.
38. **Matheny HE, Deem TL, and Cook-Mills JM.** Lymphocyte migration through monolayers of endothelial cell lines involves VCAM-1 signaling via endothelial cell NADPH oxidase. *J Immunol* 164: 6550–6559, 2000.
39. **McEver RP.** Leukocyte-endothelial cell interactions. *Curr Opin Cell Biol* 4: 840–849, 1992.
40. **Melder RJ, Munn LL, Yamada S, Ohkubo C, and Jain RK.** Selectin- and integrin-mediated T-lymphocyte rolling and arrest on TNF-alpha-activated endothelium: augmentation by erythrocytes. *Biophys J* 69: 2131–2138, 1995.
41. **Michiels C, Arnould T, Houbion A, and Remacle J.** Human umbilical vein endothelial cells submitted to hypoxia-reoxygenation in vitro: implication of free radicals, xanthine oxidase, and energy deficiency. *J Cell Physiol* 153: 53–61, 1992.
42. **Ono K, Matsumori A, Furukawa Y, Igata H, Shioi T, Matsushima K, and Sasayama S.** Prevention of myocardial reperfusion injury in rats by an antibody against monocyte chemotactic and activating factor/monocyte chemoattractant protein-1. *Lab Invest* 79: 195–203, 1999.
43. **Ozaki M, Deshpande SS, Angkeow P, Bellan J, Lowenstein CJ, Dinauer MC, Goldschmidt-Clermont PJ, and Irani K.** Inhibition of the Rac1 GTPase protects against nonlethal ischemia/reperfusion-induced necrosis and apoptosis in vivo. *FASEB J* 14: 418–429, 2000.
44. **Ozaki M, Deshpande SS, Angkeow P, Suzuki S, and Irani K.** Rac1 regulates stress-induced, redox-dependent heat shock factor activation. *J Biol Chem* 275: 35377–35383, 2000.
45. **Patel KD, Zimmerman GA, Prescott SM, McEver RP, and McIntyre TM.** Oxygen radicals induce human endothelial cells to express GMP-140 and bind neutrophils. *J Cell Biol* 112: 749–759, 1991.
46. **Prieto J, Eklund A, and Patarroyo M.** Regulated expression of integrins and other adhesion molecules during differentiation of monocytes into macrophages. *Cell Immunol* 156: 191–211, 1994.
47. **Rainger GE, Fisher A, Shearman C, and Nash GB.** Adhesion of flowing neutrophils to cultured endothelial cells after hypoxia and reoxygenation in vitro. *Am J Physiol Heart Circ Physiol* 269: H1398–H1406, 1995.
48. **Ricard I, Payet MD, and Dupuis G.** Clustering the adhesion molecules VLA-4 (CD49d/CD29) in Jurkat T cells or VCAM-1 (CD106) in endothelial (ECV 304) cells activates the phosphoinositide pathway and triggers Ca^{2+} mobilization. *Eur J Immunol* 27: 1530–1538, 1997.
49. **Ross JM, Alevriadou BR, and McIntire LV.** Rheology. In: *Thrombosis and Hemorrhage*, edited by Loscalzo J and Schafer AI. Baltimore, MD: Williams and Wilkins, 1998, p. 405–421.
50. **Sulciner DJ, Irani K, Yu ZX, Ferrans VJ, Goldschmidt-Clermont P, and Finkel T.** Rac1 regulates a cytokine-stimulated, redox-dependent pathway necessary for NF-kappaB activation. *Mol Cell Biol* 16: 7115–7121, 1996.
51. **Sundaresan M, Yu ZX, Ferrans VJ, Irani K, and Finkel T.** Requirement for generation of H_2O_2 for platelet-derived growth factor signal transduction. *Science* 270: 296–299, 1995.
52. **Sundaresan M, Yu ZX, Ferrans VJ, Sulciner DJ, Gutkind JS, Irani K, Goldschmidt-Clermont PJ, and Finkel T.** Regulation of reactive-oxygen-species generation in fibroblasts by Rac1. *Biochem J* 318: 379–382, 1996.
53. **Terada LS.** Hypoxia-reoxygenation increases $O_2^{-}\cdot$ efflux which injures endothelial cells by an extracellular mechanism. *Am J Physiol Heart Circ Physiol* 270: H945–H950, 1996.
54. **Thomas SC, Ryan MA, Shanley TP, and Wong HR.** Induction of the stress response with prostaglandin A1 increases I-kappaBalpha gene expression. *FASEB J* 12: 1371–1378, 1998.
55. **Weber C, Erl W, Pietsch A, Strobel M, Ziegler-Heitbrock HW, and Weber PC.** Antioxidants inhibit monocyte adhesion by suppressing nuclear factor-kappa B mobilization and induction of vascular cell adhesion molecule-1 in endothelial cells stimulated to generate radicals. *Arterioscler Thromb* 14: 1665–1673, 1994.
56. **Weber KS, Draude G, Erl W, de Martin R, and Weber C.** Monocyte arrest and transmigration on inflamed endothelium in shear flow is inhibited by adenovirus-mediated gene transfer of IkappaB-alpha. *Blood* 93: 3685–3693, 1999.
57. **Willam C, Schindler R, Frei U, and Eckardt KU.** Increases in oxygen tension stimulate expression of ICAM-1 and VCAM-1 on human endothelial cells. *Am J Physiol Heart Circ Physiol* 276: H2044–H2052, 1999.
58. **Yago T, Tsukuda M, and Minami M.** P-selectin binding promotes the adhesion of monocytes to VCAM-1 under flow conditions. *J Immunol* 163: 367–373, 1999.
59. **Yeh LH, Park YJ, Hansalia RJ, Ahmed IS, Deshpande SS, Goldschmidt-Clermont PJ, Irani K, and Alevriadou BR.** Shear-induced tyrosine phosphorylation in endothelial cells requires Rac1-dependent production of ROS. *Am J Physiol Cell Physiol* 276: C838–C847, 1999.
60. **Zhang S, Han J, Sells MA, Chernoff J, Knaus UG, Ulevitch RJ, and Bokoch GM.** Rho family GTPases regulate p38 mitogen-activated protein kinase through the downstream mediator Pak1. *J Biol Chem* 270: 23934–23936, 1995.
61. **Zweier JL, Kuppusamy P, and Lutty GA.** Measurement of endothelial cell free radical generation: evidence for a central mechanism of free radical injury in postischemic tissues. *Proc Natl Acad Sci USA* 85: 4046–4050, 1988.